Interface Ferroelectric Transition near the Gap-Opening Temperature in a Single-Unit-Cell FeSe Film Grown on Nb-Doped $SrTiO_3$ Substrate

Y.-T. Cui,[1] R. G. Moore,[1] A.-M. Zhang,[2] Y. Tian,[2] J. J. Lee,[1] F. T. Schmitt,[1] W.-H. Zhang,[3] W. Li,[1]
M. Yi,[1] Z.-K. Liu,[1] M. Hashimoto,[4] Y. Zhang,[4,5] D.-H. Lu,[4] T. P. Devereaux,[1] L.-L. Wang,[3,6]
X.-C. Ma,[3,6] Q.-M. Zhang,[2] Q.-K. Xue,[3,6] D.-H. Lee,[7,8] and Z.-X. Shen[1,*]
[1]*Stanford Institute for Materials and Energy Sciences, SLAC National Accelerator Laboratory, Menlo Park, California 94025, USA*
[2]*Department of Physics, Renmin University of China, Beijing 100872, China*
[3]*State Key Lab of Low-Dimensional Quantum Physics, Department of Physics, Tsinghua University, Beijing 100084, China*
[4]*Stanford Synchrotron Radiation Lightsource, SLAC National Accelerator Laboratory, Menlo Park, California 94025, USA*
[5]*Advanced Light Source, Lawrence Berkeley National Laboratory, Berkeley, California 94720, USA*
[6]*Collaborative Innovation Center of Quantum Matter, Beijing 100871, China*
[7]*Department of Physics, University of California at Berkeley, Berkeley, California 94720, USA*
[8]*Material Science Division, Lawrence Berkeley National Laboratory, Berkeley, California 94720, USA*

(Received 23 March 2014; revised manuscript received 29 September 2014; published 22 January 2015)

We report findings of strong anomalies in both mutual inductance and inelastic Raman spectroscopy measurements of single-unit-cell FeSe film grown on Nb-doped $SrTiO_3$, which occur near the temperature where the superconductinglike energy gap opens. Analysis suggests that the anomaly is associated with a broadened ferroelectric transition in a thin layer near the $FeSe/SrTiO_3$ interface. The coincidence of the ferroelectric transition and gap-opening temperatures adds credence to the central role played by the film-substrate interaction on the strong Cooper pairing in this system. We discuss scenarios that could explain such a coincidence.

DOI: 10.1103/PhysRevLett.114.037002 PACS numbers: 74.78.-w, 74.25.nd, 79.60.Jv, 77.80.bn

A single-unit cell (UC) FeSe film grown on a $SrTiO_3$ (STO) substrate exhibits a superconductinglike energy gap that persists up to 65 K [1–5], which is the highest pairing temperature in iron-based superconductors. Understanding such a substantial interface enhancement of pairing scale provides a clue of how to further enhance superconductivity in this and similar systems and can deepen our understanding of the mechanism for high-temperature superconductivity in Fe-based superconductors. Experiments using angle-resolved photoemission spectroscopy (ARPES) [2–5] have revealed that the interactions between the 1-UC FeSe film and the STO substrate play an important role in the Cooper pairing of this system. First, the strong charge transfer between FeSe and STO results in a heavily electron-doped FeSe Fermi surface, very different from a typical Fe-based superconductors [2–5]. Second, a strong coupling between the FeSe electron and STO phonon is suggested to be responsible for the enhanced Cooper pairing [5]. Here, we report new experimental evidence for the strong interaction between the FeSe film and the STO substrate, which provides further insights on the physics involved in this system.

We study high-quality single- and multiple-UC FeSe films on a Nb-doped STO substrate grown by molecular beam epitaxy (MBE). ARPES characterization reveals a gap opening near 58 K in the 1-UC sample. We then perform mutual inductance and Raman spectroscopy measurements. In both measurements, we observe an anomaly near the temperature where the gap opens. A systematic material dependence study leads us to propose that this anomaly is a broadened ferroelectric transition of the STO substrate near the FeSe/STO interface, resulting from the charge transfer and inversion symmetry breaking at the interface. The coincidence of the ferroelectric transition and the gap-opening temperature provides further evidence for the important role played by the film-substrate interaction in the Cooper pairing in the 1-UC FeSe film.

Figure 1 is the summary of the ARPES results for both 1-UC and 2-UC FeSe grown on 0.05 wt% Nb-doped STO (NbSTO). (For detailed discussions on sample growth and ARPES measurement, see Ref. [5] where the same samples have been studied.) The ARPES spectra of the 1-UC sample show that only electron bands near the Brillouin zone (BZ) corner cross the Fermi level [Figs. 1(a) and 1(b)]. In contrast, in the 2-UC spectra the hole bands around the BZ center move up and cross the Fermi level, while the bands near the BZ corner develop features that have been attributed to the tetragonal to orthorhombic structural distortion [5] [Figs. 1(c) and 1(d)]. An energy gap that opens at 58 ± 7 K (from a mean-field fitting) is observed on the electron pockets of the 1-UC film only [Fig. 1(f)]. The 2-UC film shows no sign of gap opening for all temperatures measured. Compared to that of the 2-UC film, the shift in band position in the 1-UC film indicates a significant charge transfer with the NbSTO substrate. Both the band structure and the temperature dependence of the energy gap are consistent with recent reports [2–4],

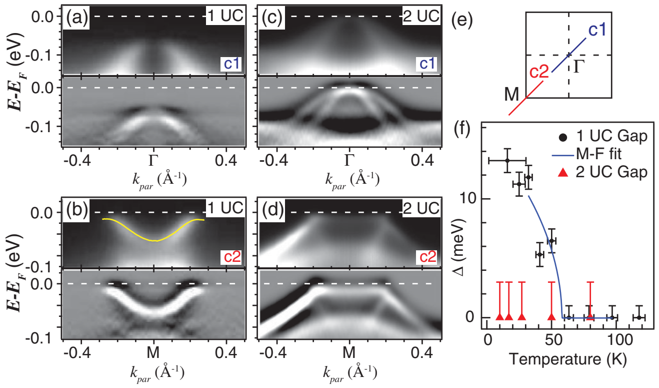

FIG. 1 (color). [(a) and (b)] The spectra of 1-UC FeSe/NbSTO. [(c) and (d)] The spectra of 2-UC FeSe/NbSTO. The locations of the moment cuts are illustrated in (e). In (a)–(d), the bottom panel is the second derivative of the raw spectrum. The white dotted lines indicate the Fermi level. The yellow solid curve in (c) is a fit of the dispersion of the electron pocket showing opening of a gap. All spectra are taken at temperature of 10 K. (e) Illustration of the Brillouin zone. (f) The extracted energy gaps as a function of temperature. The solid line is a mean-field fitting of the 1-UC gap.

suggesting a sample quality of our MBE grown films comparable to that reported by earlier studies.

Mutual inductance measurements were then performed after capping the films to study the ac conductivity response of the samples. The results for the 1-UC FeSe film are shown as the red curves in Figs. 2(a) and 2(b). An anomalous enhancement in both real and imaginary components of the mutual inductance is found to be centered around 50 K, agreeing with the ARPES gap-opening temperature within experimental uncertainties. The frequency (f) dependence [Figs. 2(c) and 2(d)] shows that in the range from 10 to 40 kHz, the mutual inductance signal is primarily in the real (dissipative) component of the transimpedance Z, which exhibits $\mathrm{Re}(Z) \propto f^2$ [Fig. 2(d)], while the weaker imaginary (inductive) component grows with frequency faster than f^2 [Fig. 2(c)]. This result suggests that the mutual inductance anomaly originates from normal metallic screening rather than superconductivity, due to the following reasons. In superconductors, the screening current is proportional to the magnetic field $B(\omega)$, due to the Meissner effect, so the measured transimpedance is expected to be primarily in the inductive channel and have a linear f dependence. In contrast, for a normal metal the induced eddy current depends on the electric field, $E(\omega) \propto dB(\omega)/dt$, thus causing signals to reside primarily in the dissipative channel with an extra power in f, consistent with our observation. The destruction of the superconducting phase is very likely due to the Se or Te capping before the mutual inductance measurement. We would like to mention that in a FeTe-capped FeSe film grown on insulating STO substrate our mutual inductance measurement showed a superconductinglike signal at temperatures below 20 K, consistent with recent reports [6,7].

To track the origin of the anomaly, we measured a series of FeSe samples with different film thicknesses and capping layers, as well as control samples without FeSe films [Figs. 2(e) and 2(f)]. We observe the following systematic behaviors: (1) all the FeSe films show a similar

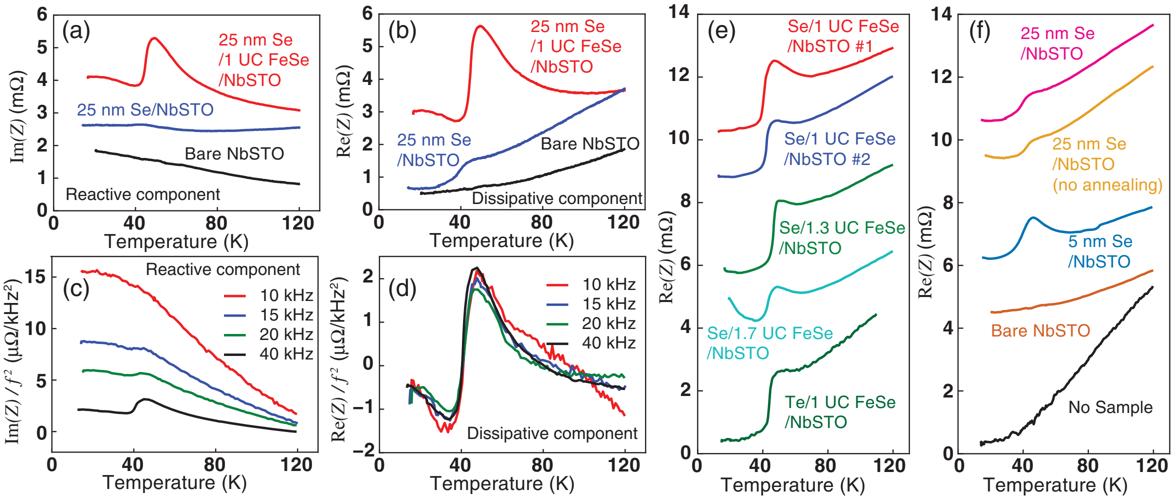

FIG. 2 (color). [(a) and (b)] Temperature dependence of the transimpedance Z measured by mutual inductance on three samples as labeled with (a) the reactive [$\mathrm{Im}(Z)$] and (b) dissipative [$\mathrm{Re}(Z)$] components. The transimpedance is taken by dividing the pickup voltage with the excitation current. The sign convention is such that an increase in the reactive (dissipative) component corresponds to an increase in the magnetic screening (dissipation) in the sample. [(c) and (d)] Normalized (c) reactive [$\mathrm{Im}(Z)/f^2$] and (d) dissipative [$\mathrm{Re}(Z)/f^2$] components of the mutual inductance measured in frequency range from 10 to 40 kHz in a 25 nm Se/1-UC FeSe/NbSTO. A linear background is subtracted in (d). (e) The dissipative components of FeSe films with different thicknesses and capping layers grown on NbSTO. The thicknesses of all capping layers are 25 nm. (f) The dissipative components of control samples without FeSe films.

50 K anomaly regardless of the film thickness and the material or thickness of the capping layer; (2) all the control samples with a capping layer but without the FeSe film also show a weaker version of the 50 K anomaly; (3) bare NbSTO does not show any anomaly. These observations have a few implications. First, the absence of the anomaly in bare NbSTO rules out that it is a bulk property of NbSTO. Second, the anomaly does not originate from the FeSe or the capping films. This leaves the possibility that the observed anomaly is an interface effect.

To examine the role of the substrate, we also performed Raman spectroscopy of 1-UC FeSe grown on 0.5 wt% Nb-doped STO (note that the Nb doping level is 10 times higher than that of the samples used in the mutual inductance measurement) in a different MBE system [1,6]. The results are shown in Fig. 3. The Raman spectra show two peaks at low wave numbers. The one labeled with red markers in Fig. 3(a), which hardens upon cooling, corresponds to an A_{1g} phonon mode [8–11]. This mode disappears above the well-known STO antiferrodistortive (AFD) structural transition temperature 105 K [12]. The second peak (labeled by the blue marker) lying very close to the A_{1g} peak has very distinct features. This mode softens upon cooling and saturates in energy at low temperature [Fig. 3(b)]. Near the transition, it exhibits an abrupt change in energy at around 50 K, approximately coinciding with the temperature where the mutual inductance anomaly occurs. This optical phonon mode is known as the ferroelectric soft mode, which is Raman inactive, but appears in the Raman spectrum due to breaking of the inversion symmetry [9,10,13–16]. The same Raman anomaly is also observed in 0.5 wt% Nb-doped bare NbSTO (i.e., without the FeSe film). However, it is not observed in undoped STO and 0.05 wt% doped NbSTO (Supplemental Material [17]). We believe the latter is due to insufficient Nb doping to produce a strong enough Raman signal (see discussions below).

We now discuss a scenario for the physics in the NbSTO substrate that can account for both the mutual inductance and Raman results. It is known that pure STO is an incipient ferroelectric (FE), which remains paraelectric with large electric susceptibility down to 0 K [19,20]. This suppression of FE transition is due to several effects. The first is the effect of competing order. STO undergoes the cubic-tetragonal AFD transition when cooled below 105 K, which allows the appearance of the A_{1g} Raman mode [8,9,11]. The AFD is a nonpolar structural distortion that suppresses the competing FE instability [21]. [See illustrations in Fig. 4(a)] The second is the effect of quantum fluctuation [19]. At lower temperatures, the FE order is further suppressed by quantum fluctuations of the dipole moments. This delicate

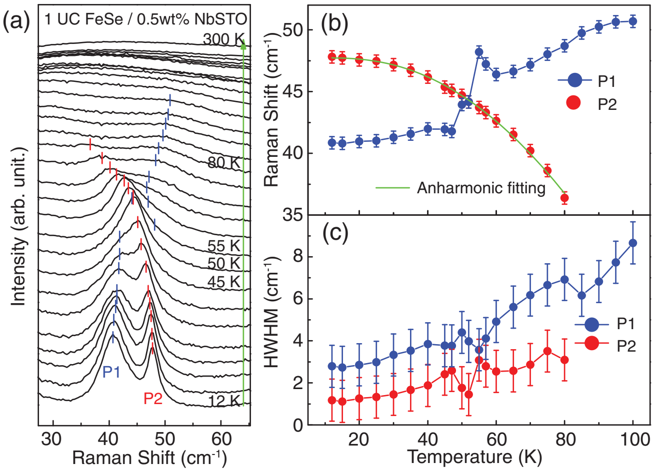

FIG. 3 (color). (a) Temperature dependence of the Raman spectra. Each spectrum is fitted with two Lorentzians plus a linear background. The fitting parameters are plotted as a function of temperature in (b) Raman shift and (c) half width at half maximum (HWHM) [18].

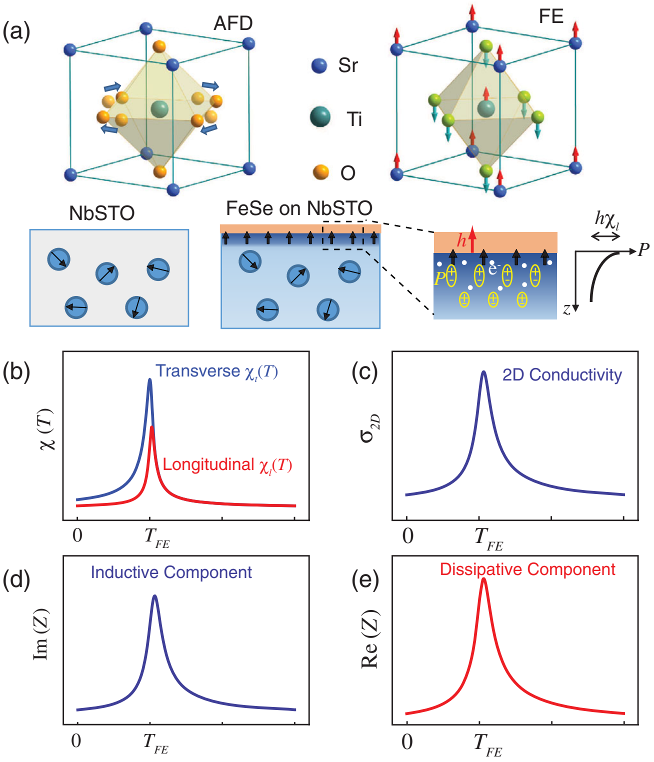

FIG. 4 (color). (a) Below 105 K, the STO undergoes an AFD transition where the TiO_6 octahedra rotate by a small amount. The blue circles indicate the micro-ordered ferroelectric regions induced by the Nb dopants. The dark blue regions indicate the surface dipole layers where excess carriers pile up due to the interface electric field between FeSe and NbSTO. The black arrows represent the induced ferroelectric dipole moments. (b) Calculated longitudinal (perpendicular to interface) and transverse (parallel with interface) electric susceptibilities in STO. (c) Calculated 2D conductivity. [(d) and (e)] Calculated transimpedance signal based on the model developed in Ref. [28] for (d) the imaginary component and (e) the dissipative component.

state is sensitive to local inversion symmetry-breaking perturbation, such as chemical doping [10,22,23], strain [24], applied electric field [8], isotope substitution [25], etc. Such inversion symmetry breaking activates the extra soft mode in Raman spectroscopy and induces local FE order [8,10,15,25–27]. Therefore, in the case of NbSTO, the observed extra Raman mode originates from the microregions around the Nb dopants. The reason it is only seen in substantially doped NbSTO is because sufficient doping is required to generate strong enough signals to be detected in a Raman experiment. When the doping level is low, these microregions do not overlap so that the AFD and local FE can coexist. The temperature dependence of the soft mode in such systems has been observed to exhibit an anomaly around the FE transition temperature—it softens upon cooling and either saturates or exhibits an upturn below the transition temperature [8,10,15]. The abrupt jump observed here might be related to the enhanced electric susceptibility and correlation length around the transition temperature (see discussions later), although its exact mechanism requires further study. In bare NbSTO, there is no net electric polarization at $T < 50$ K because the directions of local FE moments are determined by that of the local symmetry-breaking field, which varies randomly in space. In addition, the screening by itinerant electrons can also reduce the effect of the spatially random electric polarization. The Raman anomaly temperature of 50 K reflects the mean-field FE ordering temperature T_{FE} in NbSTO, when quantum fluctuations of dipole moments are suppressed by local breaking of inversion symmetry and NbSTO goes through a crossover from the paraelectric state to a state where randomly oriented FE moments exist in microregions surrounding the Nb dopants. (We note that the mean-field FE temperature for pure STO is 37 K [19] while it is also sensitive to local inversion symmetry perturbation [16,23].)

At the interface of FeSe/NbSTO, the inversion symmetry is also broken. This unidirectional symmetry breaking, largely caused by the electric field due to charge transfer, can also stabilize the underlying mean-field FE transition. Because of the unidirectional nature, a net electric polarization pointing along the surface normal should appear within a certain distance from the interface below T_{FE}. The resulting polarization gradient thus causes a space polarization charge that attracts the doped free carriers to screen it, as illustrated in Fig. 4(a). The increase in carrier density near the interface enhances the response in the mutual inductance measurement. We believe this is the root of the observed mutual inductance anomaly in films grown on NbSTO. To show that such a picture is consistent with the observed anomaly, we carry out calculations based on Ginzburg-Landau theory [29] (see the Supplemental Material [17] for details of the model). The essential results are the following: (1) the electric susceptibilities exhibit a peak around T_{FE} [Fig. 4(b)], which generally provides better dielectric screening, and (2) the dielectric screening causes excess carrier density near the interface which in turn causes the enhancement in conductivity [Fig. 4(c)]. This extra interface conductivity contributes to the screening of the electromagnetic field induced by the excitation coil and, hence, causes the anomaly in the mutual inductance around T_{FE}. The calculated mutual inductance response [Figs. 4(d) and 4(e)] agrees very well with our mutual inductance data in Fig. 2, and it also has approximately the correct frequency dependence, i.e., $\mathrm{Re}(Z) \propto f^2$, while $\mathrm{Im}(Z)$ has a higher order in f that is primarily caused by a phase shift due to the self-inductance of the film (Supplemental Material [17]). We note that the interface FE region should also contribute to the Raman anomaly. However, its thickness is likely much smaller than the probing depth of our Raman measurement (up to 4 μm due to a finite numerical aperture) such that the Raman signal primarily comes from the Nb-induced FE regions in the bulk. On the other hand, the FE regions in the bulk do not contribute to the mutual inductance anomaly because the average bulk carrier density is fixed by the doping level.

In this picture, the variation of the strength of the mutual inductance anomaly is attributed to the varying strength of the interface electric field. Compared to the Se film and bare NbSTO, the 1-UC FeSe film has substantial charge transfer with the substrate; hence, the interface electric field is much stronger, resulting in a higher concentration of free carriers and a stronger enhancement of the mutual inductance signal. We also want to point out that such an interface FE transition should also occur in films grown on undoped STO. The Nb doping simply provides the free carriers as spectators necessary to manifest the FE transition in a mutual inductance measurement.

The remaining question is why the gap-opening temperature could roughly coincide with the interface FE transition. Keeping in mind that the scale of the Cooper pairing (presumably magnetically mediated) is strongly enhanced by electron-phonon coupling [5], there are several possible explanations. (1) The interface electric field is strongly enhanced below the FE transition, which in turn strengthens such electron-phonon coupling. (2) The strong interface electric field below the FE transition causes a large change in the doping level of the FeSe film. (3) Somehow, large FE fluctuation near the FE transition helps the Cooper pairing. (4) The fluctuation of the electric dipole moment above the FE transition inhibits the Cooper pairing, and this inhibition is removed in the FE state. Scenario (1) is disfavored by the fact that the effect of electron-phonon coupling, namely, the appearance of phonon shakeoff bands, is seen at temperatures quite a bit above the mutual inductance anomaly temperature [5]. Scenario (2) is disfavored by the fact that the measured electron pocket size does not change appreciably across the anomaly temperature [3–5]. Scenario (3) would suggest that deep in the FE phase the dipole fluctuation should weaken; hence, Cooper de-pairing should occur. There is no evidence that this occurs. This discussion leaves scenario (4) as a possible explanation of the coincidence of the alleged FE transition and the gap-opening temperature. Of course, more detailed experimental and theoretical studies are required to affirm this conclusion and to address related questions of whether the general enhancement of dielectric screening in materials with ferroelectric properties is helpful for pairing.

In conclusion, we have observed an electronic anomaly in 1-UC FeSe film grown on NbSTO in both mutual inductance and Raman measurements, occurring near the energy-gap-opening temperature. We propose that this is caused by a ferroelectric transition at the FeSe/NbSTO interface. Our discussions suggest it would be interesting to search for strong pairing in systems with properties similar to that of STO but with higher ferroelectric transition temperatures or substrates that have no undesired dipole moment fluctuation but maintain the desired phononic and dielectric properties.

We thank Yayu Wang for helpful discussions. The mutual inductance work is funded by the Gordon and Betty Moore Foundation through Grant No. GBMF3133 to Z.-X.S. The MBE and ARPES work is supported by the U.S. Department of Energy, Office of Basic Energy Sciences, Division of Materials Science. ARPES measurements were performed at the Stanford Synchrotron Radiation Lightsource, a national user facility operated by Stanford University on behalf of the U.S. Department of Energy, Office of Basic Energy Sciences. D.-H. Lee is supported by the U.S. Department of Energy, Office of Basic Energy Sciences, Division of Materials Science, under Quantum Material program DE-AC02-05CH11231. L.-L. W, X.-C.M., Q.-M. Z., and Q.-K. X. are supported by Ministry of Science and Technology and National Science Foundation of China.

---

*Corresponding author.
zxshen@stanford.edu

[1] Q.-Y. Wang, L. Zhi, W.-H. Zhang, Z.-C. Zhang, J.-S. Zhang, W. Li, H. Ding, Y.-B. Ou, P. Deng, K. Chang, J. Wen, C.-L. Song, K. He, J.-F. Jia, S.-H. Ji, Y.-Y. Wang, L.-L. Wang, X. Chen, X.-C. Ma, and Q.-K. Xue, Chin. Phys. Lett. **29**, 037402 (2012).

[2] D. Liu, W. Zhang, D. Mou, J. He, Y.-B. Ou, Q.-Y. Wang, Z. Li, L. Wang, L. Zhao, S. He, Y. Peng, X. Liu, C. Chen, L. Yu, G. Liu, X. Dong, J. Zhang, C. Chen, Z. Xu, J. Hu, X. Chen, X. Ma, Q. Xue, and X. J. Zhou, Nat. Commun. **3**, 931 (2012).

[3] S. He, J. He, W. Zhang, L. Zhao, D. Liu, X. Liu, D. Mou, Y.-B. Ou, Q.-Y. Wang, Z. Li, L. Wang, Y. Peng, Y. Liu, C. Chen, L. Yu, G. Liu, X. Dong, J. Zhang, C. Chen, Z. Xu, X. Chen, X. Ma, Q. Xue, and X. J. Zhou, Nat. Mater. **12**, 605 (2013).

[4] S. Tan, Y. Zhang, M. Xia, Z. Ye, F. Chen, X. Xie, R. Peng, D. Xu, Q. Fan, H. Xu, J. Jiang, T. Zhang, X. Lai, T. Xiang, J. Hu, B. Xie, and D. Feng, Nat. Mater. **12**, 634 (2013).

[5] J. J. Lee, F. T. Schmitt, R. G. Moore, S. Johnston, Y.-T. Cui, W. Li, M. Yi, Z. K. Liu, M. Hashimoto, Y. Zhang, D. H. Lu, T. P. Devereaux, D.-H. Lee, and Z.-X. Shen, Nature (London) **515**, 245 (2014).

[6] W.-H. Zhang, Y. Sun, J.-S. Zhang, F.-S. Li, M.-H. Guo, Y.-F. Zhao, H.-M. Zhang, J.-P. Peng, Y. Xing, H.-C. Wang, T. Fujita, A. Hirata, Z. Li, H. Ding, C.-J. Tang, M. Wang, Q.-Y. Wang, K. He, S.-H. Ji, X. Chen, J.-F. Wang, Z.-C. Xia, L. Li, Y.-Y. Wang, J. Wang, L.-L. Wang, M. Chen, Q.-K. Xue, and X.-C. Ma, Chin. Phys. Lett. **31**, 017401 (2014).

[7] L. Z. Deng, B. Lv, Z. Wu, Y. Y. Xue, W. H. Zhang, F. H. Li, L. L. Wang, X. C. Ma, Q. K. Xue, and C. W. Chu, Phys. Rev. B **90**, 214513 (2014).

[8] P. A. Fleury and J. M. Worlock, Phys. Rev. **174**, 613 (1968).

[9] P. A. Fleury, J. F. Scott, and J. M. Worlock, Phys. Rev. Lett. **21**, 16 (1968).

[10] U. Bianchi, W. Kleemann, and J. G. Bednorz, J. Phys. Condens. Matter **6**, 1229 (1994).

[11] R. Ouillon, J.-P. Pinan-Lucarre, P. Ranson, P. Pruzan, S. K. Mishra, R. Ranjan, and D. Pandey, J. Phys. Condens. Matter **14**, 2079 (2002).

[12] E. Pytte and J. Feder, Phys. Rev. **187**, 1077 (1969).

[13] J. M. Worlock, J. F. Scott, and P. A. Fleury, *Light Scattering Spectra of Solids* (Springer-Verlag, New York, 1969), p. 689.

[14] J. F. Scott, Ferroelectr., Lett. Sect. **20**, 89 (1995).

[15] H. Taniguchi, T. Yagi, M. Takesada, and M. Itoh, Phys. Rev. B **72**, 064111 (2005).

[16] H. Taniguchi, M. Itoh, and T. Yagi, Phys. Rev. Lett. **99**, 017602 (2007).

[17] See the Supplemental Material at http://link.aps.org/supplemental/10.1103/PhysRevLett.114.037002 for details.

[18] Error bars are dominated by instrument uncertainties as fitting errors are much smaller.

[19] K. A. Müller and H. Burkard, Phys. Rev. B **19**, 3593 (1979).

[20] S. E. Rowley, L. J. Spalek, R. P. Smith, M. P. M. Dean, M. Itoh, J. F. Scott, G. G. Lonzarich, and S. S. Saxena, Nat. Phys. **10**, 367 (2014).

[21] W. Zhong and D. Vanderbilt, Phys. Rev. Lett. **74**, 2587 (1995).

[22] J. G. Bednorz and K. A. Müller, Phys. Rev. Lett. **52**, 2289 (1984).

[23] E. Smirnova, A. Sotnikov, R. Kunze, M. Weihnacht, O. Kvyatkovskii, and V. Lemanov, Solid State Commun. **133**, 421 (2005).

[24] J. H. Haeni, P. Irvin, W. Chang, R. Uecker, P. Reiche, Y. L. Li, S. Choudhury, W. Tian, M. E. Hawley, B. Craigo, A. K. Tagantsev, X. Q. Pan, S. K. Streiffer, L. Q. Chen, S. W. Kirchoefer, J. Levy, and D. G. Schlom, Nature (London) **430**, 758 (2004).

[25] M. Itoh, R. Wang, Y. Inaguma, T. Yamaguchi, Y.-J. Shan, and T. Nakamura, Phys. Rev. Lett. **82**, 3540 (1999).

[26] W. G. Nilsen and J. G. Skinner, J. Chem. Phys. **48**, 2240 (1968).

[27] H. Uwe, H. Yamaguchi, and T. Sakudo, Ferroelectrics **96**, 123 (1989).

[28] B. Jeanneret, J. L. Gavilano, G. A. Racine, C. Leemann, and P. Martinoli, Appl. Phys. Lett. **55**, 2336 (1989).

[29] P. Chandra and P. B. Littlewood, arXiv:cond-mat/0609347.